Fourth International Symposium on Marine Propulsors
smp'15, Austin, Texas, USA, June 2015

A Design by Optimization of Tip Loaded Propellers

Stefano Gaggero[1], Michele Viviani[2], Juan Gonzales Adalid[3], Mariano Perez Sobrino[4], Giulio Gennaro[5], Mattia Sanguinetti[6], Gianluca Bina[7]

[1,2,6,7] Department of Electrical, Electronic, Telecommunications Engineering and Naval Architecture
University of Genoa, Genoa, Italy
[3,4] SISTEMAR, Madrid, Spain
[5] SINM, Genoa, Italy

ABSTRACT

A design by optimization of tip-loaded propellers (CLT) is proposed and implemented. The approach include a parametric description of the propeller, an in-house developed Boundary Element Method (BEM) to evaluate the performances of the propellers and an optimization algorithm based on modeFRONTIER environment to drive the design process. Results for the parent propeller, in terms of both open water performances and unsteady cavitation, were validated via available experimental measurements and RANS calculations. The proposed optimized geometries are finally checked by means of dedicated RANS calculations to assess the reliability of the proposed design approach.

Keywords

Cavitation, Tip Loaded Propeller, BEM, RANS, Optimization.

1 INTRODUCTION

Energy saving is a primary objective, if not the first and probably still the most important one, in the design of marine propellers. The constant increase of oil price, the stricter regulations in terms of air pollution, and the lower limits for NOX and SOX emissions require ever more efficient designs. Nonconventional propellers, like Contracted and Tip Loaded - CLT (Gomez and Gonzales Adalid, 1992) and Kappel (Andersen et al., 2005) like geometries, represent an opportunity to increase efficiency and reduce the risk of cavitation, without the employment of completely different propulsive solutions, like contra-rotating and tandem propellers or by the adoption of ducts, stators or wake equalizers. In the last years, the interest about the application of end plates propeller in order to increase efficiency has grown, as testified by European financed projects like "Leading Edge", "Kapriccio" and "TRIPOD". De Jong et al. (1990, 1992) proposed different arrangements for the endplates extended on both the pressure and the suction side of the blade while Andersen proposed the "Kappel" concept in which the tip fin is located on the suction side of the propeller with a smooth transition between the blade and the fin itself. Specifically for Tip Loaded CLT propellers, Sanchez-Caja et al. (2006, 2012, 2014), Haimov et al. (2011), Gaggero and Brizzolara (2011), Bertetta et al. (2012a) proposed systematical calculations with RANS solvers and panel methods in order to investigate the performances, both at model and at full scale, of this type of unconventional propellers. Bertetta et al. (2012a), moreover, by means of an extensive experimental and numerical campaign, confirmed the possibility of accurate predictions of the sheet cavitation and of the downstream velocity field of CLT propellers, with particular attention to the multiple cavitating tip vortexes, through the application of potential flow solvers and RANS. More recently, Sanchez-Caja et al. (2012, 2014) presented RANS computations for the optimization of the endplate propellers through the systematic variations of the endplate geometry, in order to assess the impact of different shapes on the propeller performances. The design of the endplate is in fact a crucial point: its shape has to be studied in order to avoid unnecessary plate loading and flow separation that could negatively affect the propeller performances but, of course, it is not the only parameter that affects the efficiency of CLT propellers. As for conventional geometries, having in mind also side effects like cavitation, a better selection of pitch, camber and chord distributions (with respect to traditional lifting line/surface design approaches even if tailored for the design of unconventional geometries) can have a significant influence on the propeller performances. Moreover, for CLT propellers, the interaction between the endplate and the blade can be exploited further to improve the propeller performances. As might be expected, however, traditional design approaches cannot accurately account for all the peculiarities of Loaded Tip Propellers: potential flow approximations lack the ability to predict separation (e.g. on

the endplate) other than by means of empirical corrections; the limitations of lifting line/surface methodologies applied to such kind of geometries are much more significant. On the other hand, optimization represents a valid and versatile alternative to traditional design procedure. Exploiting the computational efficiency of the panel method together with its reliability in the prediction of CLT performances, as shown in Bertetta et al. (2012a) and Gaggero and Brizzolara (2011), it is possible to devise a design strategy in which the final design, representing a balance of different goals (e.g. efficiency and reduction of cavitation), is obtained through the systematic analysis of thousands of different propellers. Geometries are, in fact, automatically generated through a parametric description of the design table and progressively selected by the optimization algorithm based on the analysis performed by the panel method itself. This approach has been already successfully applied to conventional propellers, as shown in Bertetta et al., (2012b) and to ducted propellers, as in Gaggero et al (2012).

In present work, a design by optimization of a CLT propeller will be addressed. Starting from a CLT propeller, developed by SISTEMAR for a cruise ship and extensively tested in model scale, a new CLT propeller will be designed following the procedure previously described, to improve the efficiency and the cavitation behavior, through the systematic modification of the geometry of the blade and of the endplate. Finally a set of RANS computations will be carried out considering the final candidate geometries, with the aim to validate the design procedure. RANS calculations, whose reliability has been extensively demonstrated also for this kind of geometries, are therefore used to confirm the gains predicted by means of panel method. This final step will allow to consider effects which, as discussed before, cannot be captured by potential flow approximation, leading to the selection of the optimum CLT propeller among several optimized geometries. In addition this step, together with the comparison between numerical and experimental results for the parent geometries, will provide an insight into the necessity of including RANS codes in the design loop for this particular type of unconventional propeller.

2 FORMULATION

The numerical modeling of Contracted and Tip Loaded Propellers, from and hydrodynamic point of view is equivalent to the conventional propellers case. Once the geometry has been defined, paying special attention to the modeling of the endplate, the hydrodynamic characteristics of CLT propellers can be computed straightforward applying both potential and RANS solvers. A brief overview of the numerical approaches and of the computational setup for both the solvers is given in next sessions. The panel method has been adopted for the evaluation of steady (open water), cavitating and unsteady cavitating propeller performances. RANS, on the other hand, was used only in the simpler and less demanding case of open water propeller performances prediction, mainly as a reference for the panel method calculations carried out in the framework of the optimization. An appropriate validation of both the approaches, with respect to the available towing tank and cavitation tunnel measurements, is proposed for the original reference CLT propeller.

2.1 BEM for CLT propeller analysis

Panel/boundary elements methods model the flow field by means of a scalar function, the perturbation potential $\phi(\mathbf{x}, t)$, whose spatial derivatives represent the component of the perturbation velocity vector. Irrotationality, incompressibility and absence of viscosity are the hypotheses needed in order to write the more general continuity and momentum equations as a Laplace equation for the perturbation potential itself:

$$\nabla^2\phi(\mathbf{x}, t) = 0 \tag{1}$$

For the more general problem of cavitating flow, Green's third identity allows to solve the three dimensional differential problem as a simpler integral problem written for the surfaces (the fully wetted surface S_B, the cavitating surfaces S_{CB} and the trailing wake surface S_W) that bound the domain. The solution is found as the intensity of a series of mathematical singularities (sources and dipoles) whose superposition models the inviscid cavitating flow on and around the body (Morino and Kuo, 1974):

$$\begin{aligned} 2\pi\phi(\mathbf{x}, t) \quad &= \int_{S_B+S_{CB}} \phi(\mathbf{x}, t)\frac{\partial}{\partial \mathbf{n}}\frac{1}{\mathbf{r}}\mathrm{dS} \\ &- \int_{S_B+S_{CB}} \frac{\partial\phi(\mathbf{x}, t)}{\partial \mathbf{n}}\frac{1}{\mathbf{r}}\mathrm{dS} \\ &+ \int_{S_W} \Delta\phi(\mathbf{x}, t)\frac{\partial}{\partial \mathbf{n}}\frac{1}{\mathbf{r}}\mathrm{dS} \end{aligned} \tag{2}$$

Neglecting the supercavitating case (computation is stopped when the cavity bubble reaches the blade trailing edge) and assuming that the cavity bubble thickness is small with respect to the profile chord, singularities that model cavity bubble can be placed on the blade surface instead than on the real cavity surface (Fine and Kinnas, 1993). This approach can be addressed as a partial nonlinear approach that takes into account the weakly nonlinearity of the boundary conditions (the dynamic boundary condition on the cavitating part of the blade and the closure condition at its trailing edge) without the need to collocate the singularities on the effective cavity surface. The set of required boundary conditions for the steady problem, as usual, is:

- Kinematic boundary condition on the wetted solid boundaries,
- Kutta condition at blade trailing edge,
- Dynamic boundary condition on the cavitating surfaces,
- Kinematic boundary condition on the cavitating surfaces,
- Cavity closure condition at cavity bubble trailing edge.

Arbitrary detachment line, on the back and/or on the face sides of the blade can be found, iteratively, applying a criteria equivalent, in two dimensions, to the Villat-Brillouin cavity detachment condition, as in Mueller and Kinnas (1999). The unsteadiness of the problems, due to a non-homogeneous inflow, is solved through the application of the Kelvin theorem, as proposed by Hsin (1990). The numerical solution consists in an inner iterative scheme that solves the nonlinearities connected with the Kutta, the dynamic and the kinematic boundary conditions on the unknown cavity surfaces until the cavity closure condition has been satisfied, while an outer iterative cycle is used to integrate over the time in order to obtain a periodic solution, after the virtual numerical transient due to the key blade approach.

Viscous forces, neglected by the potential approach, can be computed following different approaches. In the first case, as proposed by Hufford (1992), a thin boundary layer solver can be coupled, through transpiration velocities, to the inviscid solution, in order to obtain a local estimation of the friction This approach, though being applied successfully for the analysis of conventional propellers, poses some problems of convergence in very off design conditions and suffers from the tip influence on streamlines on which the boundary layer calculation is performed. Consequently, in the present work a local estimation of frictional coefficient has been carried out applying a standard frictional line approach (Gonzales-Adalid et al. 2014). In particular, the VanOossanen formulation, based on local chord and thickness/chord ratio, has been employed. The discretized surface mesh consists of 1800 hyperboloidal panels per blade. The trailing vortical wake extends for five complete revolutions and it is discretized with a time equivalent angular step of 6°. With respect to conventional propellers, only a careful treatment of the radial derivatives of the perturbation potential in correspondence of the blade/endplate connection is needed.

2.2 RANS for CLT propeller analysis

The accuracy and the efficiency of RANS solvers has increased significantly in the last years, making RANSE solutions, in many engineering cases, a reliable alternative to the experimental measurements and an excellent tool to understand and visualize, for instance, the complex flow phenomena at the tip (Bertetta et al. 2012a). In addition to the panel method, that remains, thanks to its accuracy/efficiency ratio, the core of the optimization algorithm, also a commercial finite volume RANS solver, namely StarCCM+ (CD-Adapco, 2014), has been adopted to evaluate the performances and the characterizing flow features of CLT propellers. This allows to obtain, thereby, a further set of results to be compared with the experimental measures. For the non-cavitating computations, as usual continuity and momentum equations for an incompressible fluid are expressed in accordance with the Reynolds averaging, with the tensor of Reynolds stresses $\mathbf{T_{Re}}$ computed in agreement with the *Two Layers Realizable* $k-\varepsilon$ turbulence model:

$$\begin{cases} \nabla \cdot \mathbf{U} = 0 \\ \rho \dot{\mathbf{U}} = -\nabla p + \mu \nabla^2 \mathbf{U} + \nabla \cdot \mathbf{T}_{\mathrm{Re}} + \mathbf{S}_{\mathrm{M}} \end{cases} \tag{3}$$

in which $\mathbf{U}$ is the averaged velocity vector, p is the averaged pressure field, μ is the dynamic viscosity and $\mathbf{S_M}$ is the momentum sources vector. The computational domain, by means of the symmetries, is represented by an angular sector of amplitude $2\pi/Z$ around a single blade, discretized with an unstructured mesh of polyhedral cells of about 1M elements. This discretization level has been assumed valid for all the computations after numerical convergence was checked. All the simulations have been carried out as steady, using the Moving Reference Frame approach, whit SIMPLE algorithm to link pressure with the velocity fields.

3 THE ORIGINAL CLT PROPELLER

The original CLT propeller under investigation is a six-blade propeller designed for a twin-screw cruise ship by SISTEMAR S.A. The propeller has an expanded area ratio of about 0.8 and a pitch, at 0.7 r/R, of about 1.2. An overview of the original propeller geometry is given in figure 1, in which also the typical mesh arrangement, for both the panel and the RANS calculations, is represented.

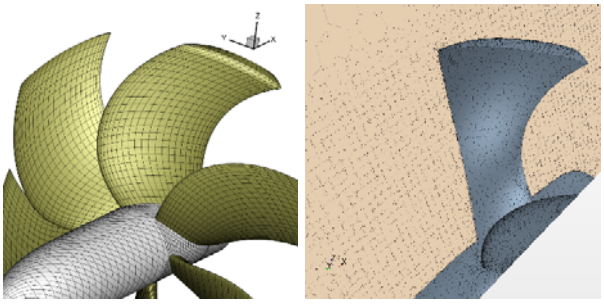

Figure 1: Original CLT propeller geometry. Details of the Boundary Element Method (left) and of the RANS (right) mesh arrangement.

The propeller was initially designed to operate in the spatial non-uniform nominal wake of figure 4 at a design thrust coefficient K_T of about 0.218 and cavitation index σ_N at shaft of about 3.5. The same functioning point has been considered for the optimization.

3.1 Validation of Open Water Performances

The preliminary analysis of the parent CLT propeller consists in open water performances calculations to assess the reliability of the Boundary Element Method in dealing with this kind of geometry. Figure 2 compares the available measurements at the towing tank with the predicted performances calculated using both the BEM and the RANS. As already evidenced in the case of similar propellers (Bertetta et al. 2012a, Gaggero and Brizzolara, 2011), calculated performances agree extremely well with measurements. For a very wide range of advance coefficient (0.4 – 0.9) differences of thrust are within 1% for the RANS and 1.5% for the BEM, with torque slightly underestimated at the lower advance coefficients by 2.5% and 4.5% respectively. Close to the zero thrust point both RANS and BEM, as usual also for conventional propeller geometries, overpredict thrust, resulting in a slightly higher open water propeller efficiency.

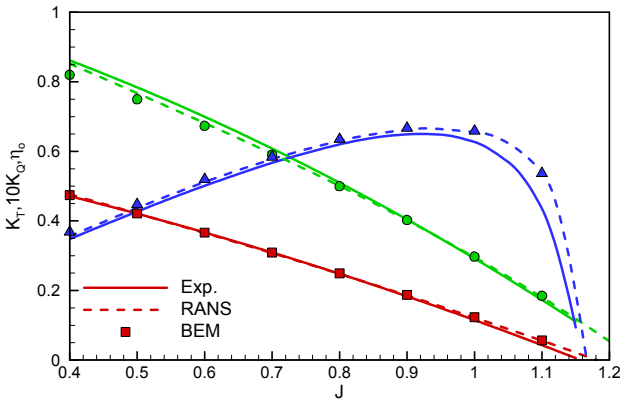

Figure 2: Original CLT propeller open water performances.

A more detailed analysis of the flow characteristics is presented in figure 3, that show the predicted pressure coefficient (in non-dimensional form with respect to the rate of rotation) on the CLT propeller blade in correspondence of higher (J = 0.5) and lower (J = 0.9) load. This kind of analysis, in addition to provide validation of the BEM code, gives an overview of the pressure field on the blade surface that will be useful to check the risk of cavitation ($-C_{PN} > \sigma_N$) by means of the RANS. The main features of the flow are similarly computed by the two methodologies. Both the numerical approaches, although with some differences, captures the influence of the endplate on the local pressure field. The increase of pressure on the face side is clear for the two loading conditions. However, while for the panel method this influence is more spread around the endplate leading edge, RANS computations show a very concentrated (more evident at higher advance values) pressure peak. These differences, obviously, can be attributed to the very different discretization level adopted for the two cases: the size of the cells around the endplate for the viscous computations are, at least, an order of magnitude smaller than the panels adopted for the inviscid computation. Moreover, a different development of the flow streamlines in proximity of the endplate, as evidenced in Gaggero and Brizzolara (2011), may play a crucial role in the pressure distribution at the tip.

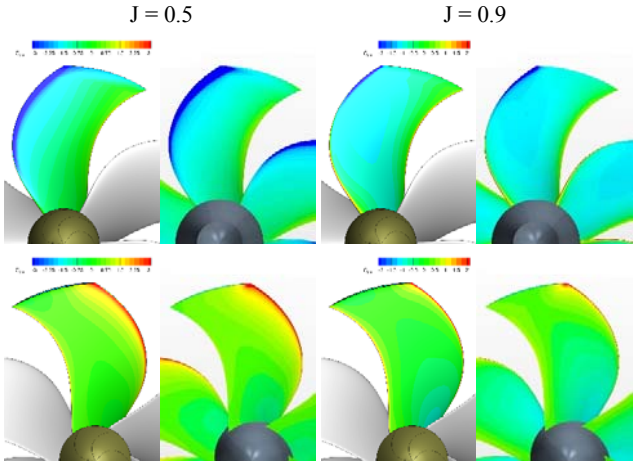

Figure 3: Comparison of pressure distributions. BEM (left) versus RANS (right).

3.2 Validation of Unsteady Cavity Extension

Unsteady cavity predictions have been validated by comparing the cavitation tunnel observed cavity extensions on the propeller operating behind a dummy model with the calculations carried out with the spatial non-uniform inflow nominal wake measured behind the same model and shown in figure 4. Only the axial component of the wake has been measured. Tangential and radial components of the velocity fields have been assumed as those due to the relative inclination between the propeller shaft and the hull stern shape (considering only an uniform vertical flow).

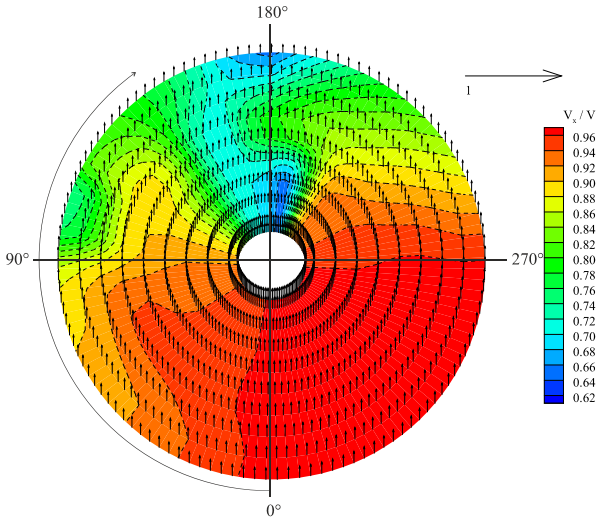

Figure 4: Nominal measured inflow and angular reference frame on the propeller disc. Starboard side (right-handed propeller) seen from aft.

The nominal wake, in which the presence of two shaft brackets is clearly visible at θ = 130° and θ = 210°, is characterized by a mean wake fraction of about 0.12. Loaded positions, due to the simultaneous action of the axial decelerated and the tangential components of the inflow spans between 160 and 270°, in correspondence of which sketches of the observed cavity extension are compared with numerical calculations, as shown in figure 5. Calculations, as usual when the effective wake is not available, have been carried out with the (mean unsteady) thrust identity assumption. A reasonable prediction of the cavity extension can be observed. Except the tip cavitating vortexes (one from the blade tip, one from the endplate tip, as already evidenced experimentally and numerically for similar geometries in Bertetta et al. 2012a) that are beyond the hypotheses of BEM approaches, sheet cavitation at blade leading edge is in agreement with respect to the experiment. A satisfactory prediction of the grow and the collapse of the bubble, passing from unloaded (130°, 250°) and loaded (180°) positions can also be observed.

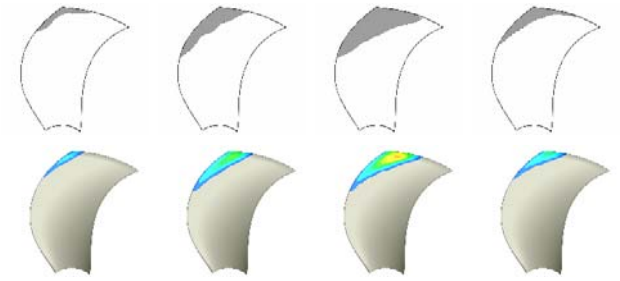

Figure 5: Observed (top) and predicted (bottom) unsteady cavity extension for the original CLT propeller.

4 DESIGN BY OPTIMIZATION

The design by optimization represents a straightforward way to overcome the limitations of conventional design tools in the case of unconventional geometries and for the satisfaction of concurrent objectives in alternative to more usual designs for "average" conditions. In present case, the original CLT propeller has been assumed as the parent geometry to derive new designs with improved cavitation behavior and efficiency. As presented in Bertetta et al. (2012b) the unsteady performances of the propeller operating in its nominal wake of figure 4 are approximated with a quasi-steady approach, as the mean of the steady performances evaluated in ''N'' angular wake sectors, whose mean flow characteristics (axial, radial and tangential distributions) are taken as the mean radial inflow for a steady computation. A fully unsteady optimization, although carried out with a panel method, is, in fact, excessively time expensive. From the unsteady analysis, actually, some information can be preliminary extracted to drive the optimization process. The most problematic angular position in terms of cavitation is almost across the 180° position, where the presence of the shaft brackets and the hull/shaftline wake causes the most decelerated inflow. On the other hand, the angularly averaged inflow is representative of the mean unsteady propeller performances, in terms of averaged thrust and efficiency. Consequently, optimizations have been carried out considering these quasi-steady conditions in order to:

1. Maximize the average (mean inflow) propeller efficiency,
2. Minimize the cavitation area at 180°,
3. Minimize the cavitation area in mean inflow condition (as a further objective oriented to cavitation optimization)
4. Deliver an average (mean inflow) propeller thrust with a ±1.5% tolerance with respect to the original design (to speed up the convergence),
5. Avoid face cavitation in any functioning conditions under investigation.

Optimization variables are represented by the parametric description of the propeller geometry, defined, as in Bertetta et al. (2012b) and Gaggero et al. (2012), by B-Spline curves approximating the CLT propeller design table. In addition, with respect to traditional geometries, CLTs requires also the parametrization of the endplate shape, with particular attention to its leading/trailing edge and its contraction line.

Two optimization cases, consequently, have been proposed. The first considers only the endplate shape to investigate its influence on cavitation and efficiency, and discuss the effectiveness of the optimization with respect to similar calculations, but carried out with a RANS solver, by Sanchez-Caja et al. (2012, 2014) for a set of different endplate shapes. Due to the limitations of the BEM, that generally suffers in the case of highly skewed panel shapes, only the endplate contraction and width have been considered for the optimization, simply scaling the leading and trailing edge endplate lines. The latter, instead, considers the blade shape in terms of pitch and camber radial distributions. Rake, skew, chord and, consequently, thickness, were maintained equal to those of the original propeller in order to avoid any considerations about blade strength in the unconventional case of Tip Loaded Propellers.

The optimization chain was built using modeFRONTIER (Esteco, 2014) and a multi-objective genetic algorithm. An initial population of 200 members, derived altering the parametric description of the original propeller within prescribed ranges, serves to feed the calculations and to derive the optimal geometries. A total of 6000 configurations in the case of the endplate optimization and of 10000 configurations in the case of the blade shape optimization have been calculated. Unfeasible designs are those not satisfying the thrust constraints.

4.1 Optimization of the Endplate

The results from the optimization of the endplate shape are summarized in the Pareto diagram of figure 6, in which geometries are collected in function of predicted mean efficiency and cavity extension at 180° position. Four propellers from the Pareto frontier (ID 1610, ID 3229, ID 8044 and ID 8309) have been selected to visualize the predicted cavity extension (by the BEM) and check the reliability of the computations by means of dedicated RANS analysis in the case of ID 1610 and ID 3229 geometries. ID 1610 and ID 3229, apparently not on the Pareto frontier in terms of cavity extension at 180°, are geometries that minimize the cavity extension when the mean inflow is considered. A rather satisfactory improvement of efficiency (up to 1.5%) and reduction of cavitation, achieved mainly on the suction side of the endplate, can be observed. These results were obtained reducing the endplate width up to the minimum value necessary to sustain the overpressure at the blade tip on the propeller face side and increasing the endplate contraction at the trailing edge up to the 96.5% of the propeller radius, as in figure 7.

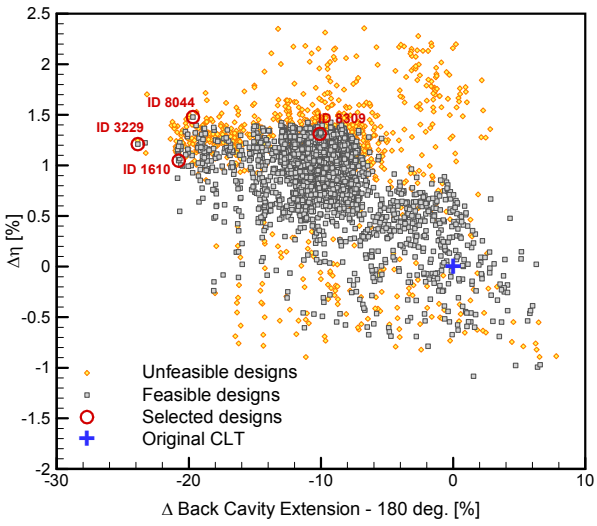

Figure 6: Pareto designs – Endplate optimization case.

RANS verification of these geometries, carried out for a set of open water conditions representative of the different inflow conditions the propeller in the non-uniform inflow is subjected to, unfortunately do not completely confirm the results of the optimization. As summarized in table 1 for ID 1610 and ID 3229, while the delivered thrust, computed with the more accurate RANS solver, lies within the design constraints, efficiency remains almost unchanged with respect to the original geometry. Moreover, ID 1610 efficiency, vice versa to BEM calculations, results slightly higher than that of ID 3229. Compared with the calculations carried out by Sanchez.Caja et al. (2012, 2014), in which RANS was able to rank different endplate contractions in

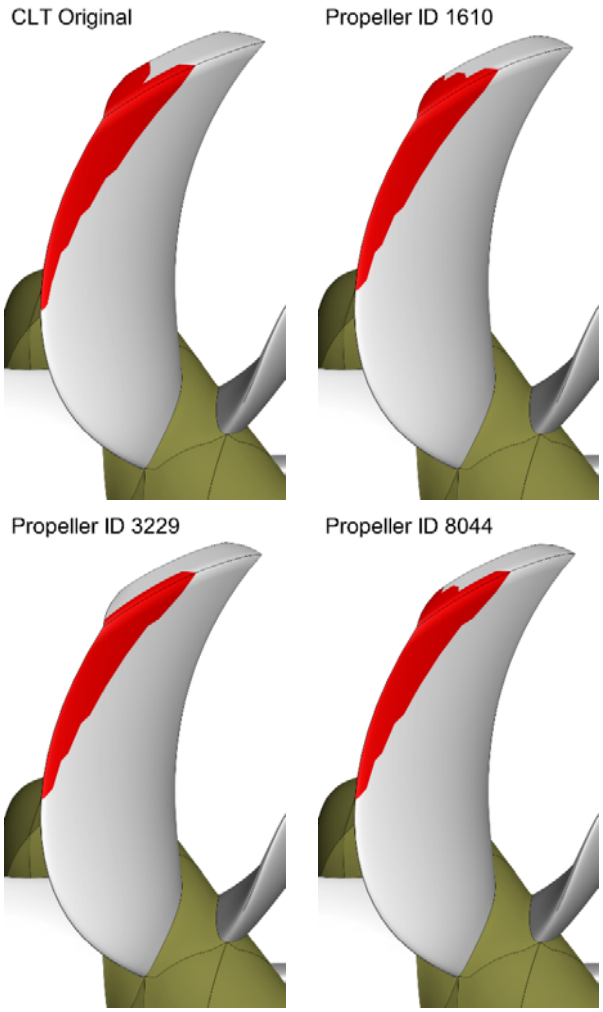

Figure 7: Predicted BEM cavity extension, 180 deg. position for the selected designs – Endplate optimization case.

terms of efficiency (with improvements of the order of few tenths of percent), the geometries obtained by the optimization process do not completely satisfy the design objective, highlighting the limitations of the BEM in dealing with very localized phenomena and viscosity effects. The analysis of the cavitating performances of the newly designed geometries is somewhat difficult at least if only iso-regions of pressure coefficient, as those of figures 8 and 9, are analyzed. For the sake of computational efficiency, actually, only RANS non-cavitating calculations have been carried out and the risk of cavitation (together with an estimation of its strength) has been evaluated only by means of the simplest cavity inception criterion $-C_{PN} = \sigma_{N\ design}$. A better estimation of the cavity extension and tip vortexes requires multiphase calculations, similar to those carried out by Bertetta et al. (2012a) already in the case of Tip Loaded Propellers and by Gaggero et al. (2014) in the case of conventional and ducted propellers cavitating tip vortexes. From the comparison of figure 8 (pressure iso-contours for the original propeller) and figure 9 (pressure iso-contours for

ID 1610 and ID 3229 geometries) only a negligible reduction of the cavity inception region at the endplate leading edge can be observed (that, however, could correspond to a reduced effective cavity extension), only partially confirming the results of the optimization.

Table 1: Summary of performances (RANS calculations) of the selected propellers. Variance with respect to open water performances of the original CLT propeller evaluated with RANS.

		ID 1610	ID 3229
J =0.7	ΔK_T	*-0.08%*	*-0.17%*
	$\Delta 10K_Q$	*-0.43%*	*-0.10%*
	$\Delta\eta_o$	*0.36%*	*-0.07%*
J =0.8	ΔK_T	*-0.01%*	*-0.21%*
	$\Delta 10K_Q$	*-0.24%*	*-0.08%*
	$\Delta\eta_o$	*0.23%*	*-0.12%*
J =0.9	ΔK_T	*0.24%*	*-0.08%*
	$\Delta 10K_Q$	*0.16%*	*0.06%*
	$\Delta\eta_o$	*0.08%*	*-0.14%*

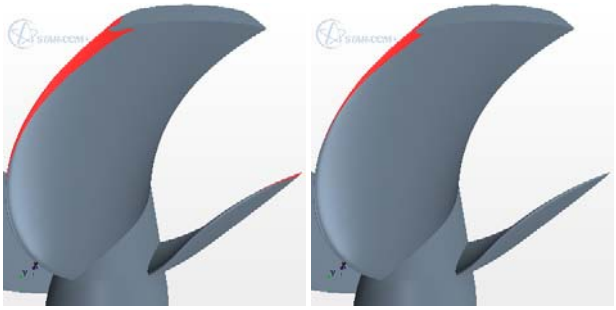

Figure 8: Original CLT propeller. Pressure iso-regions cut (RANS) at $-C_{PN} = \sigma_{N\,design}$ at J = 0.7 (left) and J = 0.8 (right). $\sigma_{N\,design} = 3.5$.

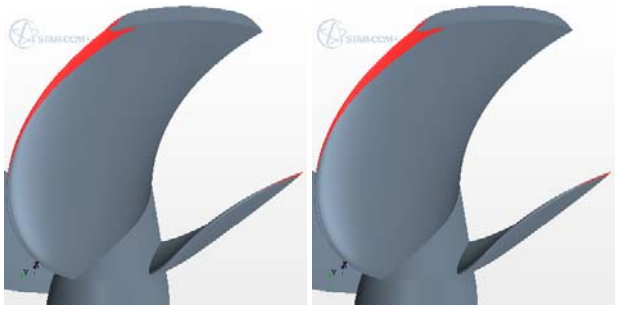

Figure 9: ID 1610 (left) and ID 3229 (right) pressure iso-regions cut (RANS) at $-C_{PN} = \sigma_{N\,design}$ at J = 0.7. $\sigma_{N\,design} = 3.5$.

4.2 Optimization of Propeller Blade Shape

A more confident optimization consists in the variation of the blade shape by means of a parametric change of the pitch and the maximum camber radial distribution, as proposed in this second design run. To maximize the results of the optimization, even if the influence of variation of the endplate shape predicted by the BEM turns out to be overestimated the contraction line of propeller ID 3229 (minimization of the endplate cavitation) has been adopted for all the newly designed propellers. This assumption, consequently, neglects the mutual influence between the endplate and the propeller blade shape. Results of the design are summarized, again, in a Pareto diagram and are reported in figure 10. The shape of the blade is much more effective for the reduction of the predicted cavity extension with respect to the endplate alone, with optimal designs achieving an outstanding reduction up to 70% of the cavitating area of the original CLT propeller. Apparently efficiency is only slightly sacrificed due to an obvious unloading of the outer propeller sections to improve the cavitating behavior of the optimal geometries, with reductions, predicted by the BEM, lower than 1% in the case of the higher improvements in terms of cavitating behavior. A detailed analysis, by the BEM, of the performances of a set of four new geometries belonging to the Pareto frontier (ID 11644, ID 12219, ID 20024 and ID 21058) is shown in figure 11, in which the predicted cavity extensions in correspondence of the quasi-steady condition at 180° are compared with the original CLT propeller operating in the same conditions.

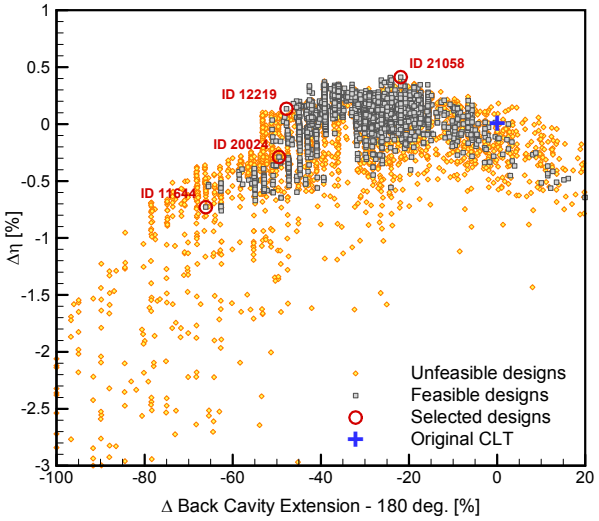

Figure 10: Pareto designs – Blade optimization case.

RANS calculations, even if limited to non-cavitating conditions, have been finally carried out, for the four selected propellers, to assess the optimization results. As in the previous design run, only open water performances and iso-regions of $-C_{PN} = \sigma_{N\,design}$ have been considered for the comparison. However, a set of different advance coefficients were calculated to cover, at least in terms of equivalent working conditions, the functioning point observed by the propellers in unsteady conditions. Results, summarized in

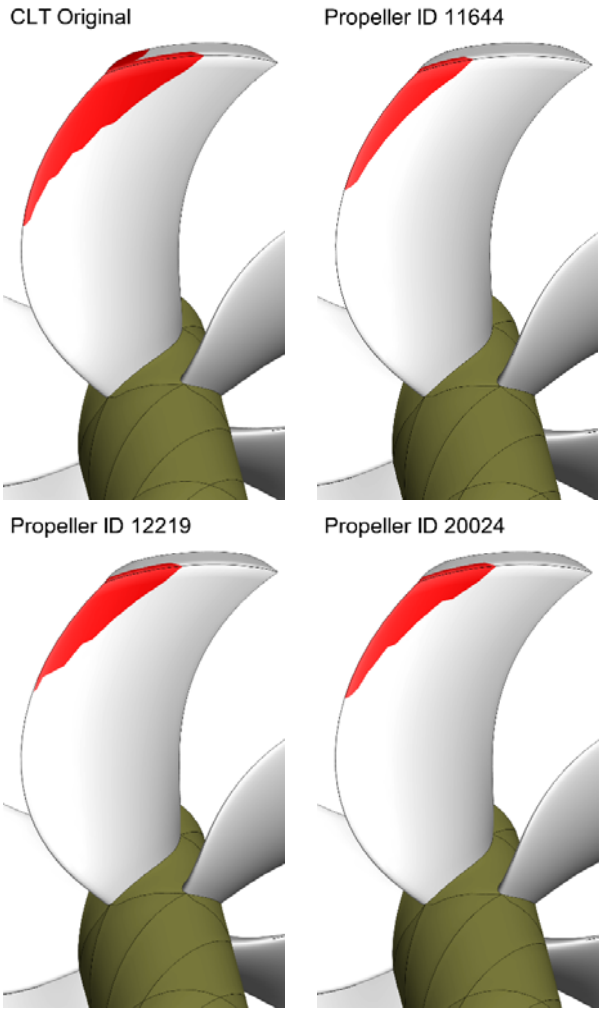

Figure 11: Predicted BEM cavity extension, 180 deg. position for the selected designs – Blade optimization case.

table 2, are encouraging. First, the design assumption of a thrust coefficient constrained within ±1.5% with respect to the original CLT performances is confirmed, again, by the more accurate viscous calculations for almost all the four propellers under investigations. The design advance coefficient in the non-uniform nominal wake of figure 4 is close to 0.8, in correspondence of which only tenth of percent of variance can be appreciated for ID 20024 and ID 21058. Only at higher advance coefficients, for which the comparison of the predicted performances by the BEM and by the RANS already showed some higher discrepancies, the design constraint (effectively applied only in correspondence of the mean inflow working point) is not completely satisfied, with an increase of propeller thrust, however, limited to 3% in the worst case. On the other hand the predicted efficiency for all the propellers is slightly higher than that of the original geometry. This result, opposite to that obtained by the BEM in the optimization loop (and partially in disagreement with the tendency of the BEM/RANS results highlighted in the previous design exercise), emphasizes the natural limitations of panel method in dealing with such very specific problems and in accurately ranking geometries on the basis of calculations that lie within the interval of confidence of the methodology, even if in this case the result was better than expected.

Table 2: Summary of performances (RANS calculations) of the selected propellers. Variance with respect to open water performances of the original CLT propeller evaluated with RANS.

		ID 11644	**ID 12219**	**ID 20024**	**ID 21058**
J =0.7	ΔK_T	*0.65%*	*0.59%*	*1.27%*	*1.42%*
	$\Delta 10K_Q$	*-0.88%*	*-0.37%*	*-0.06%*	*1.01%*
	$\Delta\eta_o$	*1.54%*	*0.97%*	*1.33%*	*0.41%*
J =0.8	ΔK_T	*1.41%*	*0.78%*	*1.89%*	*1.74%*
	$\Delta 10K_Q$	*0.43%*	*0.21%*	*0.97%*	*1.51%*
	$\Delta\eta_o$	*0.98%*	*0.58%*	*0.91%*	*0.23%*
J =0.9	ΔK_T	*2.79%*	*1.19%*	*3.01%*	*2.40%*
	$\Delta 10K_Q$	*2.24%*	*1.00%*	*2.40%*	*2.29%*
	$\Delta\eta_o$	*0.53%*	*0.19%*	*0.59%*	*0.11%*

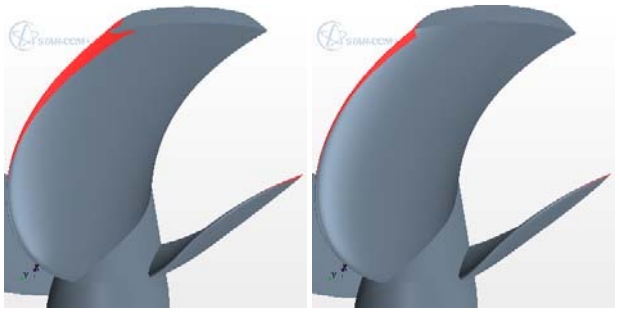

Figure 12: Original CLT (left) and ID 11644 (right) pressure iso-regions cut (RANS) at $-C_{PN} = \sigma_{N\,design}$ at J = 0.7. $\sigma_{N\,design} = 3.5$.

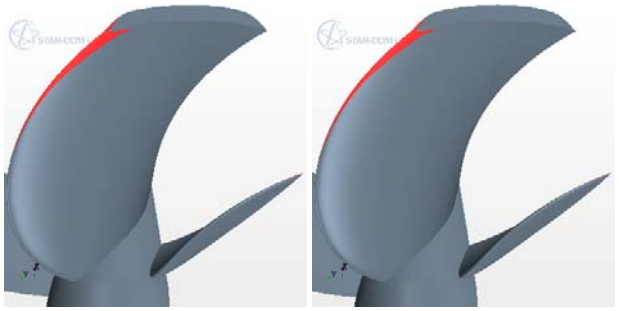

Figure 13: ID 12219 (left) and ID 20024 (right) pressure iso-regions cut (RANS) at $-C_{PN} = \sigma_{N\,design}$ at J = 0.7. $\sigma_{N\,design} = 3.5$.

The analysis, based on the simplified cavity criterion proposed in figures 12 and 13, in addition, proves the effectiveness of the proposed design approach. Even if the comparison is limited to the extension of regions having a pressure below the vapor tension, the reduction of the cavitation risk achieved with the optimal design is evident.

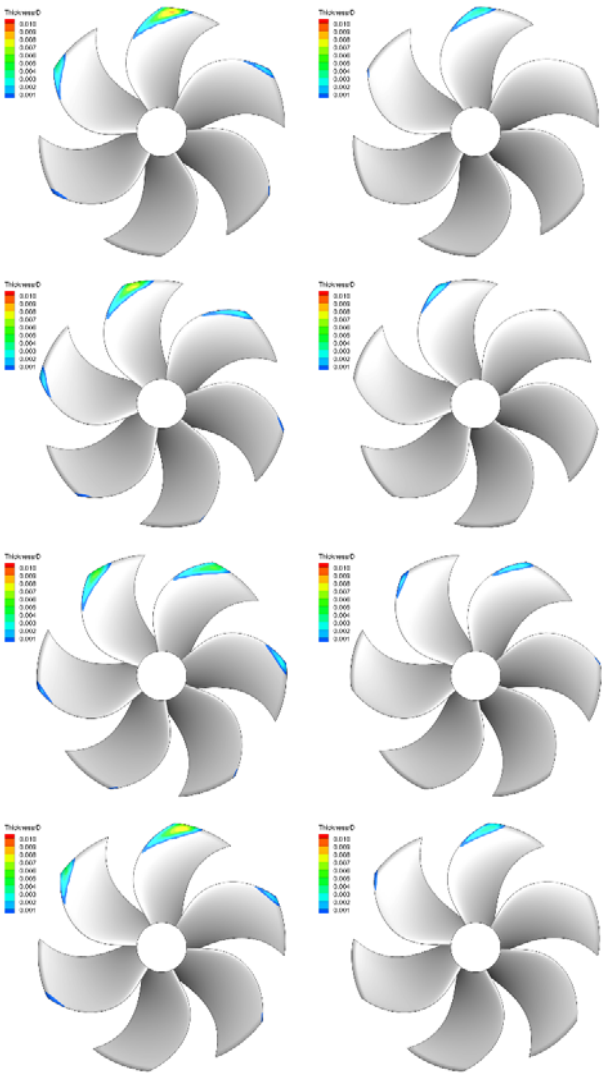

Figure 14: Predicted BEM cavity extension at different angular positions. Original CLT (left) versus ID 11644 (right).

In particular, in the case of propeller ID 11644, identified by the optimization as the geometry with the maximum reduction of the cavity extension, also RANS calculations show a considerable improvement of the cavitating performances of the propeller. Moreover for the other two geometries of figure 13, characterized, from the BEM point of view (see, for instance, figures 10 and 11), by a very similar cavitation development, RANS predictions show the same trend, with a cavity inception extension similar and slightly higher than that of the ID 11644 configuration, as pointed out in the optimization. Finally, the performances of the ID 11644 geometry have been analyzed in fully unsteady conditions to have a direct comparison with the original CLT performances partially validated via the experimental observations of section 3.2. Results are summarized in figure 14. The improvements achieved with the newly designed propeller are evident. The developed laminar cavity bubble on the ID 11644 configuration has a significantly lower extension and thickness, appreciable both in term of chordwise and radial bubble extension for a given blade angular position and in terms of range of angular positions in correspondence of which the blade is subjected to cavitation. Even if the prediction of tip cavitating vortexes is beyond the possibility of the panel method (and having in mind the typical double tip vortex CLT propellers are subjected to), the thinner cavity bubble at blade tip, together with a globally unloaded blade, could be a sign of a retarded tip cavitating vortexes, especially in the case of tip vortexes from laminar sheet cavitation. A thinner and less extended cavity bubble means, moreover, a reduced cavitation volume that, in principle, is related to propeller induced pressures. Propeller ID 11644 could grant, also from this point of view, improved performances with respect to the parent geometry. Its mechanical performances predicted by the BEM in fully unsteady conditions, are in line with those of the original propeller. The delivered mean unsteady thrust is only slightly lower (-0.5%) with respect to the required one, confirming the reliability of the quasi-steady approach adopted for the optimization of the propeller geometry.

5 CONCLUSIONS AND FUTURE WORK

A design by optimization of Contracted and Tip Loaded propellers was proposed and implemented. Results, both in terms of predicted propeller open water performances and unsteady cavitation using a BEM code, were first validated against the available measurements and observations at the towing tank and at the cavitation tunnel. The satisfactory agreement between experiments and computations allows the application of the Panel Method as the core of a design process based on optimization in which, further to usual efficiency criteria, also cavitation is considered, aiming to its reduction. Preliminary applications of the proposed design approach were carried out starting from an available parent propeller geometry. Designs from the optimization runs were analyzed and compared by means of dedicated RANS analyses aimed to validate the design assumptions (thrust constraints, quasi-steady approach) and the entire design chain based on BEM calculations. Results, in the case of blade shape optimization, were satisfactory: predicted performances by the Panel Method largely agree with the RANS calculations and the final geometries proved to be able to grant similar performances with a significantly lower extension of the cavity bubble. However, some limitations of the design chain, related to the assumption Panel Method are based on, were highlighted during the analysis. BEM calculations, in the particular case of efficiency, have a confidence interval that does not allow for a reliable and robust ranking of very similar geometries, resulting in differences between BEM and RANS calculations of the order of about 1.5%, that may be considered acceptable for

this kind of application, in view of a final choice by means of RANS calculations. On the contrary, in this particular case, when cavitation is taken into account, the well-proven reliability of the Panel Method allows for a valid selection of the optimal geometries. A final unsteady analysis confirmed furthermore the design assumptions and highlighted once more the improved performances of the newly designed propeller. On the light of these preliminary results the design by optimization, already successfully proposed by the authors in the case of conventional and ducted propellers, turns out to be a valid and promising approach to deal with unconventional geometries, constraints and objectives at least within the limitations of the Panel Method. A careful investigation on the influence of different geometrical parameters (chord and skew, for instance) to achieve even better unsteady performances has to be carried out. Furthermore, a careful validation of alternative viscous approaches to be included into BEM calculations (i.e. thin boundary layer coupling) should be conducted in order to extend this approach directly in full scale, in correspondence of which CLT propellers achieve their best performances due to a positive interaction with the boundary layer itself.

REFERENCES

Andersen, P., Friesch, J., Kappel, J.J., Lundegaard, L., Patience, G. (2005). "Development of a Marine Propeller with Nonplanar Lifting Surfaces". Marine Technology, Vol. 42 (3), pp. 144-158.

Bertetta, D., Brizzolara, S., Canepa, E., Gaggero, S. and Viviani, M. (2012a). "EFD and CFD Characterization of a CLT Propeller". International Journal of Rotating Machinery, Volume 2012, Article ID 348939.

Bertetta, D., Brizzolara, S., Gaggero, S., Savio, S. and Viviani, M. (2012b). "CPP propeller cavitation and noise optimization at different pitches with panel code and validation by cavitation tunnel measurements". Ocean Engineering, Vol. 53, pp. 177-195.

CD-Adapco, (2014). "StarCCM+ 9.04.009 Users Guide".

Esteco S.r.l. (2014). "ModeFRONTIER 2014 Users Manual".

Fine, N. E., and Kinnas, S. A. (1993), "A Boundary-Element Method for the Analysis of the Flow around 3-D Cavitating Hydrofoils," J. Ship Res., 37(3), 213-224.

Gaggero, S., Tani, G., Viviani, M. and Conti, F. (2014). "A study on the numerical prediction of propellers cavitating tip vortex". Ocean Engineering, Vol. 92, pp. 137-161.

Gaggero, S., Brizzolara, S. (2011). "Endplate Effect Propellers: a Numerical Overview". Proc. of the Sustainable Maritime Transportation and Exploitation of Sea Resources: IMAM 2011, Genova, Italy.

Gaggero S., Rizzo C.M., Tani G. and Viviani M. (2012). "EFD and CFD design and analysis of a propeller in decelerating duct". International Journal of Rotating Machinery, Volume 2012, Article ID 823831

Gómez, G.P. and González-Adalid, J. (1992). "Tip Loaded Propellers (CLT) - Justification of their Advantages over Conventional Propellers Using the New Momentum Theory". SNAME 50th Anniversary, (1942-1992).

Gonzales-Adalid J., Perez Sobrino M., Garcia Gomez A., Gennaro G., Gaggero S., Viviani M. and Sanchez-Caja A. (2014). "Comparison of different scaling methods for model tests with CLT propellers". 11th International Conference on Hydrodynamics, Singapore.

Haimov, H., Vicario, J., Del Corral, J. (2011). "RANSE Code Application for Ducted and Endplate Propellers in Open Water". Proc. of 2nt International Symposium on Marine Propulsors, Hamburg, Germany, June 2011.

Hsin, C.Y. (1990). "Development and analysis of Panel Methods for Propellers in Unsteady Flows". Ph.D. dissertation, Massachusetts Institute of Technology.

Hufford, G.S. (1992). "Viscous flow around marine propellers using boundary layer strip theory". Ph.D. dissertation, Massachusetts Institute of Technology.

Jong, K. de and Sparenberg, J.A. (1990). "On the Influence of Choice of Generator Lines on the Optimum Efficiency of Screw Propellers". Journal of Ship Research, Vol. 23, No. 2, pp. 79-91.

Jong, K. de, Sparenberg, J.A., Falcão de Campos, J.A.C. and van Gent, W. (1992). "Model Testing of an Optimally Designed Propeller with Two-Sided Shifted End Plates on the Blades". 19th Symposium on Naval Hydrodynamics, Seoul, August 1992.

Morino, L. and Kuo, C.C. (1974). "Subsonic Potential Aerodynamic for complex configuration: a general theory". AIAA Journal, Vol. 12, pp. 191-197.

Mueller, A.C. and Kinnas, S.A. (1999). " Propeller sheet cavitation predictions using a panel method". Journal of Fluids Engineering, Vol. 121, pp. 282-288.

Sánchez-Caja, A., Sipilä, T., Pylkkänen, J. (2006) "Simulation of the Incompressible Viscous Flow around an Endplate Propeller Using a RANSE Solver". 26th Symposium on Naval Hydrodynamics, Rome, Italy, 17-22, 2006.

Sánchez-Caja, A., Gonzales-Adalid, J., Perez-Sobrino, M. and Saisto, I. (2012). "Study on End-Plate Shape Variations for Tip Loaded Propellers Using a RANSE Solver". 29th Symposium on Naval Hydrodynamics, Gothenburg, Sweden, 2012.

Sánchez-Caja, A., Gonzales-Adalid, J., Perez-Sobrino, M. and Sipilä, T. (2014). "Scale effects on tip loaded propeller performance using a RANSE solver". Ocean Engineering, vol. 88, pp. 607-61

DISCUSSION

Question from Stefano Brizzolara

It would be interesting to show how the pitch and camber distributions change on the optimized propeller with respect to the original distributions. Please include these data in the reply.

What is the wake pitch distribution you used for the optimization cases? Does it depend on the design variant geometry? Do you expect that a fully aligned wake would change the results of the optimization?

Authors' Closure

Thank you for your observation. For what regards the first question, unfortunately, we have to fulfill a non-disclosure agreement that force us not to explicitly show the propellers geometry. In order to appreciate the results of the optimization approach, however, the percentage variations of the pitch and the camber distributions of two of the optimized geometries (i.e. ID11644 and ID12219) with respect to the original geometry are shown in figures I and II. Even if only non-dimensional, these distributions show how the optimization works to improve the propellers cavitating behavior while maintaining almost unvaried the delivered thrust. Pitch is generally unloaded, especially at the tip where the optimized propellers achieve the higher improvements in terms of cavitation, while camber is significantly increased for both the geometries.

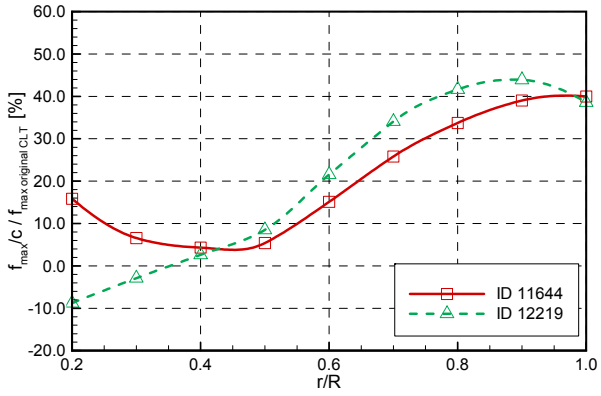

Figure I: Variation of the maximum camber distribution with respect to the original propeller geometry. ID11644 and ID 12219 optimized propellers.

For what regards the propeller wake model, in present calculations a frozen wake approach has been used. The pitch of the propeller vortical trailing wake is a weighted mean between the hydrodynamic pitch and the geometrical pitch of the blade. In particular, the trailing vortical wake detaches from the blade trailing edge with the geometrical pitch and it is gradually blended with the far wake that, instead, is an helicoid surface with the hydrodynamic pitch.

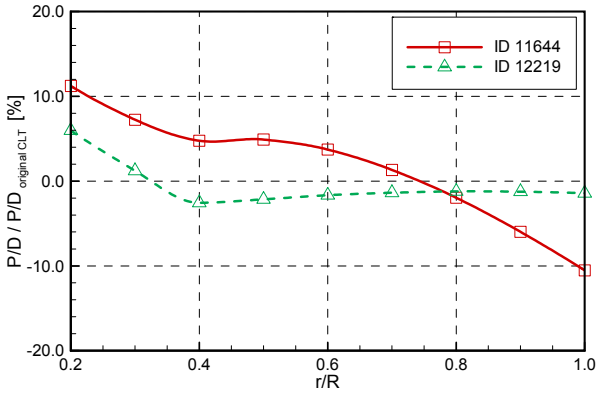

Figure II: Variation of the pitch distribution with respect to the original propeller geometry. ID11644 and ID 12219 optimized propellers.

In that respect, the trailing wake depends on the optimization process that alters the blade pitch distribution to achieve better propeller performance. In the framework of the optimization process, this approach has been preferred to a fully numerical wake alignment algorithm in order to save the computational time required for the iterative process that drives the alignment of the vortical wake. When compared to the experimental measures, the satisfactory results that have been achieved with the frozen wake model justify its adoption for present calculations.

The proposed Boundary Element Method, however, can deal with the fully wake alignment. An example of calculation is proposed in figure III. The original CLT propeller is considered in uniform inflow, at an advance coefficient equal to 0.9. In table I, in addition, the predicted thrust and torque coefficients with the frozen wake model (the one adopted during the optimization process) and with the fully aligned wake model are compared.

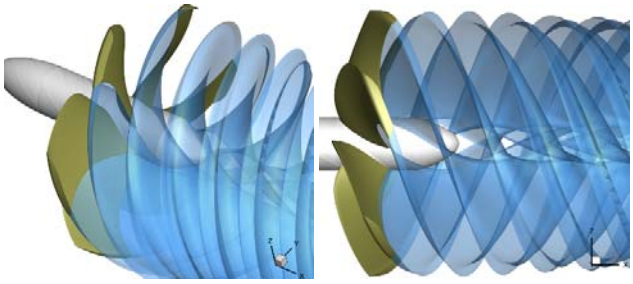

Figure III: Fully aligned wake for the original CLT propeller at J = 0.9.

The wake alignment algorithm reasonably predicts the typical roll-up of the vortexes from the endplate of the CLT propeller. The vortex from the endplate tip has, as observed experimentally and numerically predicted with RANSE in Bertetta et al. (2012a), a lower pitch with respect to the pitch of the vortex from the endplate root. The interaction between

these two vortexes results in a rollup of one vortex over the other, well foreseen also by the wake alignment model of the Panel Method. In terms of predicted forces, the influence of a fully aligned wake, at least close to the design point, seems almost negligible, as summarized in table I, confirming the reliability of the frozen wake model adopted in the optimization process.

In off-design conditions, however, when the average between the geometric and the hydrodynamic pitch is no more a reliable approach to model the trailing vortical wake, the fully aligned wake model could represent an important feature also for CLT propellers.

Table 2: Predicted propeller performance with the numerical fully wake alignment.

J	**$K_{T\ fix.\ wake}$**	**$K_{T\ aligned}$**	**$10K_{Q\ fix.\ wake}$**	**$10K_{Q\ aligned}$**
0.8	0.248	0.245	0.493	0.490
0.9	0.186	0.184	0.395	0.392